Develop Automated Oxide-Aperture Size Measurement for GaAs VCSELs

Zetai Liu, Haonan Wu, Derek Chaw, Milton Feng

Department of Electrical and Computer Engineering, University of Illinois at Urbana-Champaign
Nick Holonyak Micro and Nanotechnology Laboratory, 208 N Wright St, Urbana, IL, 61801

Email: mfeng@illinois.edu

Keywords: Automated Measurement, Oxide-Confined microcavity VCSEL, Full-Sample Characterization

Abstract

An accurate automated measurement system for oxide apertures during the VCSEL (Vertical-Cavity Surface-Emitting Laser) fabrication process has been successfully developed. This automation is employed for process control monitoring and has been demonstrated to achieve an accuracy rate exceeding 94%, and a significant reduction in process cycle time. Furthermore, it offers the added benefit of enabling wafer-scale characterization throughout the oxide-confined VCSEL fabrication process. The study also delves into the intricate relationships between VCSEL laser spectrum, threshold values, oxide-aperture size, and the optical mode cavity, particularly when scaling down the cavity size.

INTRODUCTION

Oxide-confined VCSELs, are pivotal semiconductor devices with a wide range of applications across various fields, including data communication and LiDAR technology. Their reputation is built upon their reliability, extremely low threshold, and outstanding high-speed performance, as documented in [1], [2]. The escalating demand for data storage and communication in data centers, the proliferation of connected devices, and advancements in cryogenic temperature technologies have made optical data links an increasingly attractive option for data transmission in data centers and other industries [3].

Additionally, optical data links currently offer a cost-effective solution with high bandwidth capacity, minimal power consumption, and superior connectivity when compared to electronic links. With these surging demands and continuous technological innovations, the VCSEL market, particularly the oxide-confined VCSEL segment, has garnered substantial interest across industries. It presents an opportunity for high-speed optical data links that are not only cost-effective but also energy-efficient on a per-bit basis [2]. Our previous research has successfully demonstrated the viability of VCSEL data links at cryogenic temperatures [4], [5] and room temperature[6].

However, to achieve large-scale uniform production of oxide-confined VCSELs, several challenges must be addressed. One of the most prominent issues is the lack of uniformity and control over the oxide aperture during the wet thermal oxidation process in fabrication [2]. Previous studies have underscored the critical relationship between the size of the oxide aperture in oxide-confined VCSELs and their overall performance [7], [8], [9]. The oxide aperture serves the dual purpose of confining both the electrical current and the optical mode within VCSELs [9]. Variations in the size of the oxide aperture directly impact VCSEL properties such as the threshold current (I_{TH}), maximum output power, differential resistance, modal characteristics, and other relevant device attributes [1], [7], [9]. These variations inevitably lead to disparities in device performance. Consequently, the precise and comprehensive measurement of the oxide aperture dimensions for every individual device on a processed wafer holds paramount importance during the VCSEL fabrication process.

DEVELOPMENT OF NEW CRYOGENIC VCSELS FOR HIGH-SPEED DATA LINK

Following the successful establishment of a data link at 2.6 K using cryogenic VCSELs in 2021 [4] and achieving a PAM-4 optical data link rate exceeding 50 Gbps in 2022 [5], our research has continued to explore ways to enhance the optical communication performance of VCSELs by reducing the size of the oxide aperture. Drawing from studies conducted on room temperature VCSELs, it is evident that reducing the oxide aperture size should result in a decrease in the VCSELs' threshold current, consequently lowering the energy cost per bit [4], [5], [7]. Furthermore, microcavity lasers have demonstrated higher bandwidth capabilities while consuming less power, thanks to the phenomenon of Purcell enhancement [10]. This enhancement is poised to significantly improve VCSELs' high-speed performance. Consequently, we have set our target oxidation diameter at approximately 2 µm, in contrast to the previously reported 6.8 µm [4], [5].

However, challenges have arisen due to non-uniform airflow within the wet oxidation chamber and the reduced target size for the oxide aperture. Achieving sample uniformity has become a primary concern. Moreover, for VCSELs featuring oxide aperture sizes smaller than 3 µm, even a minute difference of 0.5 µm in the size of the oxide aperture can lead to more significant variations in device properties when compared to our prior work with 6.8 µm

devices [9]. Therefore, to gain a comprehensive understanding of microcavity VCSEL device performance in relation to its physical characteristics, particularly under cryogenic temperatures, it is imperative to accurately characterize the oxide aperture sizes at a wafer scale.

DEVELOPMENT OF AUTOMATED OXIDATION APERTURE MEASUREMENT

Previously, oxide apertures were manually measured using ImageJ, which was a time-consuming process, especially when characterizing the entire wafer. Consequently, only 20 oxidation monitors were selected randomly from the pool of over 300 measurable oxidation monitors on the wafer to estimate the average oxide aperture size for the devices. Unfortunately, basing device qualification on this average value sometimes led to misleading conclusions. To enable complete wafer characterization, we established a complete workflow with optimized measurement and detection parameters in an OpenCV based environment.

The images of all oxidation monitors were acquired manually using a microscope system under 940 nm IR backlight. Figure 1 (a) displays an oxidation monitor image collected via the microscope system. After processing, the identified boundary of the oxide aperture is delineated by a black circle, as illustrated in Figure 1 (b). This circle serves as a direct reference for later measurement accuracy evaluation. In this specific example, the micro-cavity oxide aperture size is measured to be 1.77 µm. Figures 1 (c) and (d) present SEM images of processed devices after wet oxidation, further illustrating the mesa structure.

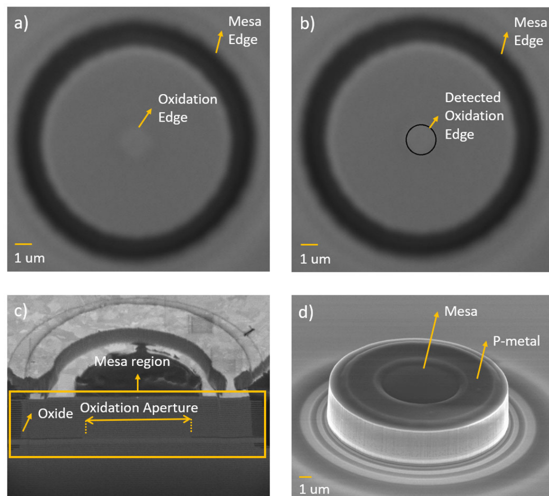

Fig. 1. (a). oxidation monitor image under IR backlight. (b) processed oxidation monitor image with labeled detected oxidation edge and Microcavity size aperture of 1.77 um was determined. (c). SEM image of cross-section view of fabricated GaAs VCSEL under FIB, with oxide-aperture of 6.8 µm. (d). SEM image of device after p-DBR mesa etch and oxide-aperture steps.

Following the processing of the collected images of oxidation monitors, the measurement accuracy of all the data was assessed using the same criteria as manual measurements. Subsequently, an oxidation wafer map was generated. Figure 2 showcases an example of an oxidation wafer map after measurement. It is evident that the oxidation aperture size for the 15 µm diameter mesa oxidation monitor predominantly varies between 2 to 3 µm, with a few outliers for this specific wafer. Additionally, the distribution of oxidation appears to be largely unexplainable and unpredictable after analyzing the wafer map of the four samples. This emphasizes the importance of characterizing the entire wafer and possible misleading conclusion drawn in previous measurement techniques.

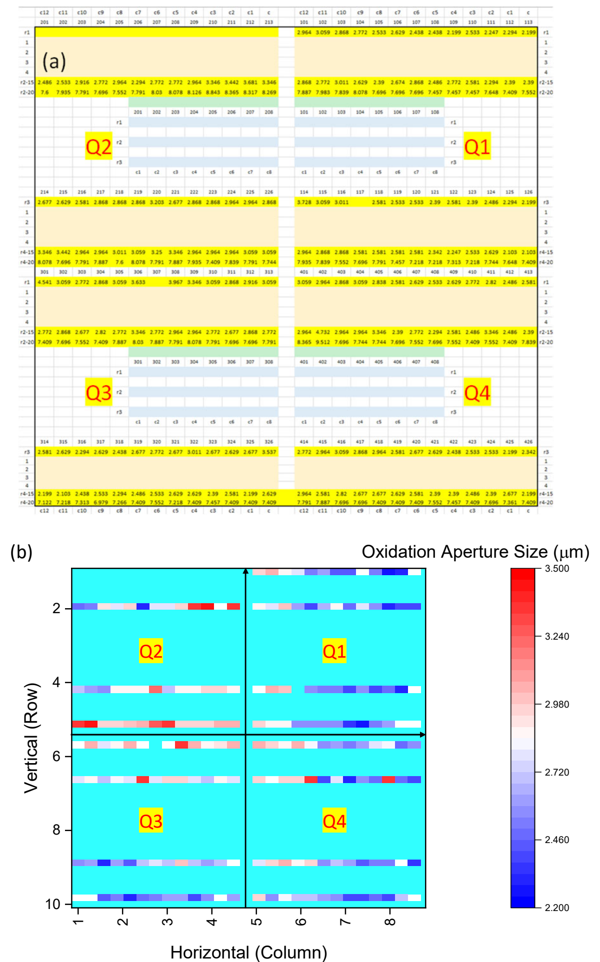

Fig. 2. a). complete oxidation map in table. b). complete oxidation map in heat map. Yellow cells indicate measured oxidation dummy location on sample. Data of top panel oxidation monitor in Q2 are missing due to device fabrication issue which make them unmeasurable.

In this process lot, a total of 1027 oxidation monitors were measured across four different ½ inch by ½ inch samples. Fourteen of these monitors were not detectable by the program, and 43 were categorized as detection errors, with 30

of them having an aperture size smaller than 2 μm. This suggests a preference for larger oxidation aperture diameters. The reason for this preference in aperture size can be attributed to the non-circular shape of the oxidation aperture with smaller sizes, as demonstrated in Figure 3. This preference arises because the current technique uses a predefined circular boundary to expedite measurements. No noticeable preferences in the location of oxidation monitors within the image were observed. The processing rate of this automated process has been measured to exceed 100 images per minute, a substantial improvement compared to the previous manual measurements, which were conducted at a rate of approximately 1 to 2 images per minute. The final successful detection rate was calculated to be 94.45%.

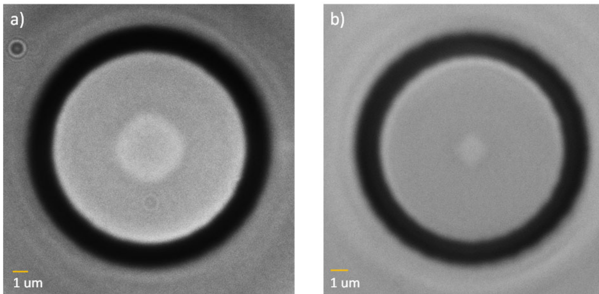

Fig. 3. Comparison of (a) Large oxide-aperture (circular-like) and (b) Small oxide-aperture (non-circular-like).

Implementation of automated program to microcavity cryogenic VCSEL analysis

Our CryoVCSELs exhibit remarkable versatility by operating effectively within a broad temperature range, spanning from room temperature down to an impressive 2.9K. The successful implementation of this precise automated oxide-aperture measurement technique has empowered us to confidently characterize the relationship between CryoVCSEL threshold current (I_{TH}) and oxide-aperture size (area). In theory, one would anticipate a decrease in I_{TH} as the oxide-aperture size is reduced from the previously reported 6.8 μm to 2 μm. However, the data we collected did not support this expected trend. One plausible explanation for this unexpected outcome could be associated with the fact that the optical cavity size of the laser differs from the size of the oxide aperture as it scales down towards a microcavity. We were able to determine the optical cavity size by analyzing the measured laser spectrum mode spacing. As depicted in Fig. 4., when plotting I_{TH} against the Optical Mode Aperture Area, it became apparent that there is a critical point where I_{TH} approaches a minimum value of approximately 0.75 mA at room temperature and 0.20 mA at 2.9K, as the area of optical cavity aperture is reduced to zero.

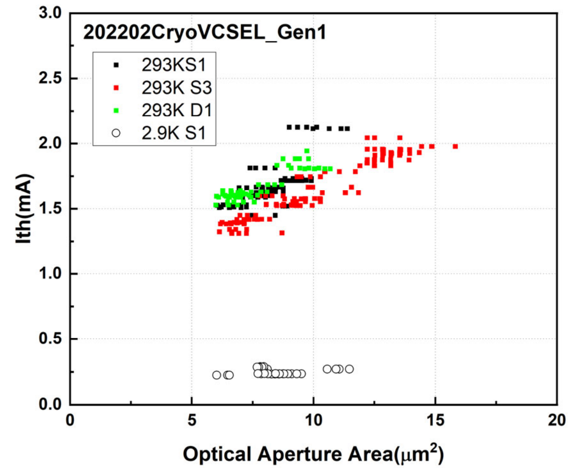

Fig. 4. Measured CryoVCSEL laser threshold vs optical aperture area which is different than oxide-aperture size.

Conclusions

In this work, we have demonstrated the implementation of automated oxide-aperture measurement technique by OpenCV. This technical approach provides us with wafer scale oxidation aperture characterization capability. This capability could help us to better understand VCSEL performance with relates to its physical properties. Additionally, it could provide us with insight of wafer scale oxidation variation within chamber, which helps in increase fabrication uniformity and improve process control. At the same time, at 2.9 K, for microcavity VCSELs, oxide aperture size differs from calculated optical-cavity size.

Acknowledgements

This work was supported by Dr. Mark Becker (IARPA), Dr. Michael Gerhold (ARO), and Dr. William Harrod (IARPA) on Develop Ultralow Power Cryo-VCSELs for 4K Fiber Data Link under ARO Grant No. W911NF-22-1-0229. We also appreciate the support from IntelliEpi for MOCVD material growth epitaxial layers.

References

[1] M. Feng, C.-H. Wu, and N. Holonyak, “Oxide-Confined VCSELs for High-Speed Optical Interconnects,” *IEEE J Quantum Electron*, vol. 54, no. 3, pp. 1–15, Jun. 2018, doi: 10.1109/JQE.2018.2817068.

[2] B. D. Padullaparthi, “VCSEL Industry: Prospects and Products,” in *VCSEL Industry: Communication and Sensing*, wiley, 2021, pp. 47–71. doi: 10.1002/9781119782223.ch3.

[3] D. Wu, W. Fu, H. Wu, and M. Feng, “Cryogenic VCSEL microwave-optical model for laser frequency response prediction and e-h

recombination lifetime analysis," *J Appl Phys*, vol. 132, no. 22, Dec. 2022, doi: 10.1063/5.0127575.

[4] H. Wu, W. Fu, M. Feng, and D. Deppe, "2.6 K VCSEL data link for cryogenic computing," *Appl Phys Lett*, vol. 119, no. 4, Jul. 2021, doi: 10.1063/5.0054128.

[5] W. Fu, H. Wu, and M. Feng, "Superconducting Processor Modulated VCSELs for 4K High-Speed Optical Data Link," *IEEE J Quantum Electron*, vol. 58, no. 2, Apr. 2022, doi: 10.1109/JQE.2022.3149512.

[6] H. Wu, D. Wu, X. Yu, and M. Feng, "Developing Single-Mode VCSEL for Extending High-Speed PAM4 Transmitting Distance in SMF-28 Fiber Up to 1 km and 70 °C."

[7] A. M. Sharizal *et al.*, "Effect of oxide aperture on the performance of 850 nm vertical-cavity surface-emitting lasers," *Optik (Stuttg)*, vol. 120, no. 3, pp. 121–126, Jan. 2009, doi: 10.1016/j.ijleo.2007.07.005.

[8] F. Adel Ismael Chaqmaqchee and J. A. Lott, "Impact of oxide aperture diameter on optical output power, spectral emission, and bandwidth for 980 nm VCSELs," *OSA Contin*, vol. 3, no. 9, p. 2602, Sep. 2020, doi: 10.1364/osac.397687.

[9] M. Liu, M.-K. Wu, and M. Feng, "Optimization of Selective Oxidation for 850 nm (IR) and 780 nm (Far-red) Energy/Data Efficient Oxide-Confined Microcavity VCSELs."

[10] F. Tan, C. H. Wu, M. Feng, and N. Holonyak, "Energy efficient microcavity lasers with 20 and 40 Gb/s data transmission," *Appl Phys Lett*, vol. 98, no. 19, May 2011, doi: 10.1063/1.3589363.

ACRONYMS

VCSEL: Vertical-Cavity Surface-Emitting Laser
I_{TH}: Threshold Current of VCSEL
SEM: Scanning Electron Microscope
FIB: Focused Ion Beam
OpenCV: Open-Source Computer Vision Library
LIV: Light, Voltage versus Current Curve